

# 6 Tribology Project

## – Photon and Quantum Basic Research Coordinated Development Program –

*Project Leader: Hideki Seto*

### 6-1. Introduction

Tribology is the science of interacting surfaces in relative motion including the study and application of the principles of friction, lubrication and wear. It is closely related to our everyday life, in diverse areas from live cell friction to mechanical parts lubrication and seismology. It is estimated that the reduction of energy consumption by the optimization of friction and lubrication is worth 1.3 trillion yen in Japan, and thus it is important to understand both the industrial applications and fundamental science of tribology. Elemental processes of phenomena can occur at various spatial scales from angstrom to km, and the phenomena are essentially non-equilibrium. Additionally, the phenomena occur at buried interfaces and are difficult to observe in situ. For these reasons, fundamental aspects remain unsolved, both theoretical and experimental.

In this project, we intend to utilize neutrons and muons to investigate friction and lubrication, because these probes are powerful tools for in-situ investigation of buried interfaces, and are complementary methods to observe the dynamical behavior of molecules and molecular assemblies.

### 6-2. Development of magnetic marker $\mu$ SR method for probing molecular dynamics

Energy dissipation in rubber materials is closely related to the local dynamics of atoms/molecules on polymer chains. When stress is applied to rubber, part of the energy is stored as elastic energy and the rest may dissipate through a variety of channels including local atomic or molecular motions, or both, causing energy loss. Controlling this kind of energy loss is one of the key issues in

the development of rubbers such as low-fuel consumption tires.

The characteristic time scale (frequency) of polymer dynamics ranges from  $10^0$  to  $10^{12}$  Hz and so it is important to obtain information on dynamical behaviors by various experimental techniques having different time windows, such as neutron scattering, acoustic sound attenuation, dielectric relaxation and viscosity measurement. However, there is a gap in the specific time range of these conventional experimental techniques, which can be covered by muon spin rotation/relaxation ( $\mu$ SR). Thus,  $\mu$ SR could be a unique tool to probe the dynamical behavior of rubbers through the channel of spin fluctuation.

The objective of this project is to obtain information on the polymer dynamics over the specific frequency region mentioned above, where the characteristic time scale presumably corresponds to the local atomic or molecular motions. Accordingly, we chose polybutadiene (PBD) rubber as the prototype polymer system and performed  $\mu$ SR measurements.

The local electronic state of muon (muonium (Mu) or diamagnetic muon) is identified by measurements under a transverse magnetic field (TF). It was inferred from the fast Fourier transformation (FFT) of the TF- $\mu$ SR time spectra that the signal consists of diamagnetic muon and Mu components (see the report of FY2015). Here, we focus on the diamagnetic component from which we expect to obtain information about the slow dynamics in the  $\sim$ MHz region.

The diamagnetic component at ambient temperature (AT) in PBD exhibits extremely weak depolarization which is virtually unaffected by external longitudinal fields (LF). This makes it difficult to obtain information on molecular dynamics

by the conventional  $\mu$ SR method, because the hyperfine field  $H_d$  at the muon site may be too small to reflect its time evolution ("motional narrowing"), i.e.,  $\gamma_\mu H_d \ll \nu$ , where  $\nu$  is the characteristic frequency for the dynamics in question and  $\gamma_\mu$  is the muon gyromagnetic ratio ( $2\pi \times 135.53$  MHz/T). More specifically, since the depolarization rate is approximately given by the Redfield form

$$\lambda \sim \frac{2\delta_\mu^2 \nu}{\omega_\mu^2 + \nu^2},$$

where  $\delta_\mu = \gamma_\mu H_d$  and  $\omega_\mu = \gamma_\mu H_0$ , with  $H_0$  being the external LF, it also suggests that  $\omega_\mu \ll \nu$  given experimental conditions. In order to cope with such circumstances, we proposed the magnetic marker method, where a small amount of fine magnetic particles (= magnetic markers) introduced into the polymer matrix serves to generate an additional hyperfine field for the nearby muons. Since these magnetic markers are presumably bound to the surrounding polymer molecules, there is a possibility that the additional hyperfine fields from marker particles, which are fluctuating due to polymer dynamics, may bring the associated muon depolarization into the sensitive time range for  $\mu$ SR.

To establish this magnetic marker method, we took a two-step approach: we first performed a series of  $\mu$ SR measurements to optimize the concentration and size of the fine magnetic particles in pristine PBD. Then we proceeded to measure the optimal content of magnetic markers incorporated into more realistic materials including PBD with vulcanization (cross-linked) and/or with fillers [carbon black (CB)].

### 6-2-1. Optimization of magnetic markers

Considering that the hyperfine fields from magnetic markers (dipolar fields) are short-range, there is a trade-off between the sensitive range of dynamics (both in spatial and time ranges) and the possible influence of the marker itself on the molecular dynamics in increasing the concentration/size of marker particles. We adopted a guiding principle that the concentration and particle size should be minimized as long as the  $\mu$ SR spectra retain significant sensitivity to the dynamics.

We first performed  $\mu$ SR measurements under a variety of marker concentrations and sizes to optimize the marker condition regarding the

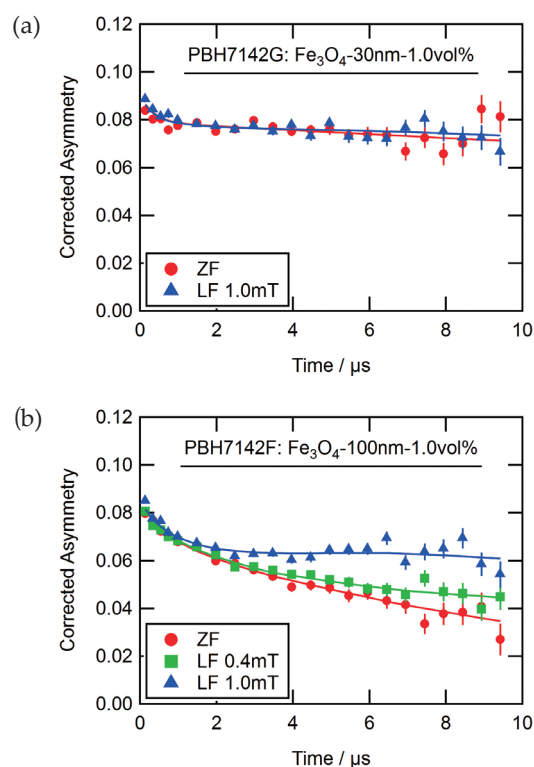


**Fig. 1:**  $\mu$ SR time spectra of marker-introduced PBD samples corrected at AT and under LF. Particle sizes of the marker are (a) 100 nm and (b) 30 nm, with 1.0 vol% concentration.

magnitude of depolarization rate. We adopted magnetite (Fe<sub>3</sub>O<sub>4</sub>) in powder form (fine particles) as a marker. The magnetite powder was introduced into PBD samples with several particle sizes [100–500 nm (labeled 500 nm), 50–100 nm (100 nm), and 20–30 nm (30 nm)] with two different concentrations (0.1 vol% and 1.0 vol%).

For the samples with the concentration of 0.1 vol%, the time spectra exhibited little change compared with those for the pristine PBD regardless of marker size [close to the spectra shown in Fig. 1(a)]. Meanwhile, for the samples with 1.0 vol%, those with 100 nm [Fig. 1(b)] and 500 nm markers exhibited significant variation, while that with 30 nm marker remained unchanged [Fig. 1(a)]. Considering that the observed depolarization rate is large enough to probe dynamics in detail, we adopted the marker size of 100 nm and concentration of 1.0 vol% for the study of practical rubber materials.

### 6-2-2. Magnetic marker $\mu$ SR in realistic materials

To manipulate the molecular dynamics in PBD, we prepared four PBD rubber samples

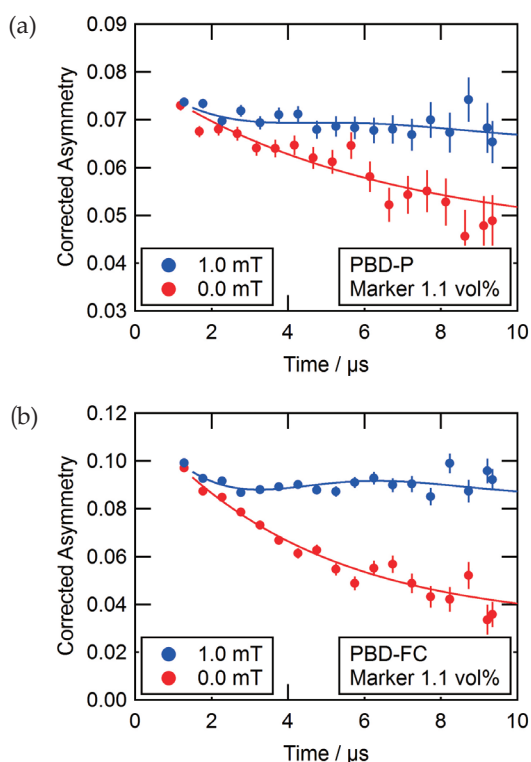


**Fig. 2:**  $\mu$ SR time spectra of marker-introduced PBD samples corrected at AT and under LF. Marker particles with the size of 100 nm and concentration of 1.1 vol% are introduced into (a) pristine PBD and (b) PBD with cross-linking and filler.

with/without cross-linking and with/without CB filler. The 100 nm magnetic marker was also introduced with the concentration of 1.1 vol%. The obtained time spectra for (a) pristine PBD sample and (b) PBD sample with cross-linking and filler are shown in Fig. 2. Since the muon hyperfine field is presumed to be common between these two samples, the difference in the LF dependence of the time spectra is due to that in the fluctuation rate of the hyperfine field. The stronger LF dependence for the rubber sample with cross-linking and CB filler indicates that the fluctuation rate is lower than that of pristine PBD rubber. We used a dynamical Kubo-Toyabe function for the least-squares curve fits to analyze the obtained time spectra. The obtained fluctuation frequency  $\nu$  is shown in Table 1. The frequency of the sample with cross-linking and filler is 0.05 MHz, which is slower than that of pristine PBD (0.12 MHz).

Here, we discuss the origin of the observed fluctuation. The particle size of 100 nm is much larger than that of PBD polymer chains. Therefore, it is likely that the motion of marker particles is negligible in the time scale of  $\mu$ SR. On the other hand, provided that a muon is stuck (either

physically or chemically) to a polymer chain, its position will fluctuate with the polymer motion. Thus, the fluctuation frequency of the muon can be regarded as that of the polymer itself. Finally, we conclude that the magnetic marker  $\mu$ SR method has been demonstrated to be feasible by showing that introducing the cross-linking and filler slows down the polymer dynamics on a microscopic scale.

**Table 1.** Relation between obtained fluctuation rate  $\nu$  and conditions of sample with cross-linking and filler.

Sample	PBD	PBDC	PBDF	PBDFC
Cross-linking	–	○	–	○
Filler	–	–	○	○
$\nu$ /MHz	0.12(3)	0.08(1)	0.06(1)	0.05(1)

## 6-2. Structure and mechanical properties of elastomer thin films bound to carbon interface

Interfaces between polymers and inorganic materials are of pivotal academic and industrial interest. An example is the interphase in nanocomposites, a class of materials composed of polymers (matrix) and inorganic nanopowders (fillers). In general, the performance of a nanocomposite strongly depends on not only the physical properties of the matrix but also the interaction between the matrix and the filler material. It is noteworthy that the physical response of a composite can be modulated via the interactions resulting from the attachment/detachment of polymers to fillers. This means that an understanding of the interfaces between the polymer matrix and inorganic fillers is essential to construct highly functionalized nanocomposites.

A specific example is tire materials; because the rubber used for tires consists mainly of a polymer elastomer matrix and carbon black fillers, an understanding of the interface between the polymer and carbon is important for improving quality. A nanometer-thick layer, the so-called bound rubber layer (BRL), is typically formed on the carbon material surfaces and is resistant to dissolving even in a good solvent. In theory, the interactions between polymers and carbon material surfaces restrict molecular motion, which correlates with increased resistance to mechanical deformation as compared to free polymers that are located away from the carbon material surface.

Great effort has been made in industry to manufacture high-performance tires by making

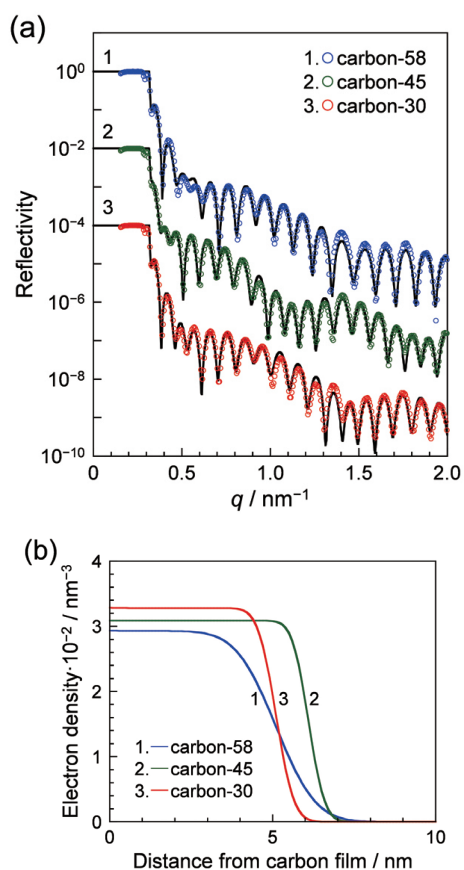


**Fig. 3:** X-ray reflectivity of RL on carbon film. Solid curves show calculated reflectivities on the basis of model electron density profiles shown in panel (b).

a surface-modified filler. As the structure and/or thermal molecular motion of the polymer at the filler/polymer interface is affected by the interactions with the filler, it is believed that surface modification changes the properties of the BRL, resulting in improved tire performance. However, this is still hypothetical, because there is insufficient evidence and empirical data, e.g., on the influence of surface modification on the BRL. The relationship between the BRL and tire performance needs to be evaluated to develop guiding principles for improving tire performance. Although the number of reports on the general BRL framework is increasing, it is still unclear how the surface modification of fillers affects the structural and mechanical properties of BRLs. To answer this fundamental but industrially crucial question, we performed hydrophilization treatment of carbon to change the surface free energy, and investigated the influence on the structure and mechanical properties of an elastomer bound to the surface, model BRL.

To do this, we adopted a model system of the interface, namely a PBD thin film on a carbon layer was prepared. To extract BRL, the films

were rinsed with toluene and well dried at room temperature prior to the measurement.

Figure 3(a) shows the scattering vector ( $q = (4\pi/\lambda) \cdot \sin\theta$ , where  $\lambda$  and  $\theta$  are the wavelength and the incident angle of X-ray, respectively) dependence of X-ray reflectivity (XR) for a BRL on DLC film. Open symbols denote experimental data, and solid curves are calculated reflectivity based on model electron density ( $\rho_e$ ) profiles shown in Fig. 3(b). For clarity, each data set for the BRL is offset by two decades. Since the calculated reflectivities were in good agreement with the experimental data, it can be considered that the model ( $b/V$ ) profiles well reflect the density profiles of the bilayer along the direction normal to the surface.

Interestingly, the obtained  $\rho_e$  of the BRL changed systematically with the surface property:  $\rho_{e1}$  on carbon-58, i.e., the hydrophilic carbon, was the smallest, while that on carbon-45 was intermediate, and that on carbon-30, i.e., the hydrophobic carbon, was the largest. Indeed, several simulations and theoretical works predict that the interaction can change the density of a matrix in the vicinity of a filler surface: a decrease in density is predicted for non-adsorptive surfaces, while an increase in density is predicted for strongly adsorptive surfaces.

Table 2 summarizes the film thickness ( $h$ ) and mass density ( $\rho$ ) of BRL.

**Table 2.** Film thickness and density of the BRLs.

	$h/\text{nm}$	$\rho/\text{g}\cdot\text{cm}^{-3}$
BRL (carbon-58)	6.3	0.88
BRL (carbon-45)	7.4	0.92
BRL (carbon-30)	6.6	0.98

$\rho$  was calculated from  $\rho_e$  by:

$$\rho = \rho_e M \cdot \left\{ N_A \sum (n_i z_i) \right\}^{-1}$$

where  $N_A$  and  $M$  are the Avogadro number and molecular weight, respectively.  $n_i$  and  $z_i$  are the number of atoms and the atomic number of element  $i$ , respectively. Whereas the  $\rho$  value of BRL on carbon-58 was smaller than that of the bulk, those of BRL on carbon-45 and carbon-30 were larger. Notably, the  $\rho$  value of BRL on carbon-30 was  $0.98 \text{ g}\cdot\text{cm}^{-3}$ , approximately 10% larger than that of the bulk. Provided PB maintains the glassy state even at room temperature (297 K),  $\rho$  can be estimated to be  $0.98 \text{ g}\cdot\text{cm}^{-3}$  from the thermal expansion coefficient and the density in the

glassy state. The increase in the mass density of the BRLs leads to a decrease in the free volume of the molecules, and the suppression of thermal molecular motion. In other words, the suppression of thermal motion because of the interaction with the carbon surface could change the density of the BRLs.

To further examine the influence of surface modification on the mechanical properties, we used atomic force microscopy (AFM) to investigate Young's modulus of the BRLs. Figure 4 shows the force-distance curves of the BRLs. In the case of the BRL on carbon-58, the normal force slightly increases immediately after contact with the RL surface on approach, the slope becomes gradually steeper with closer contact, and the force curve presents a large hysteresis upon retraction. This suggests that the cantilever first detected the normal force of the BRL, which has a thickness of 6.3 nm in the rubbery state; it then detected that of the carbon under the BRL upon further contact, and finally detected that modulated by the rubbery BRL adhesion upon retraction. In contrast, the slope of the force-distance curves immediately increased for the BRLs on carbon-45 and carbon-30. The slopes of carbon-45 and carbon-30 were less than that of the carbon film but obviously more than that of the rubbery PBD, and were comparable to that of the glassy polystyrene

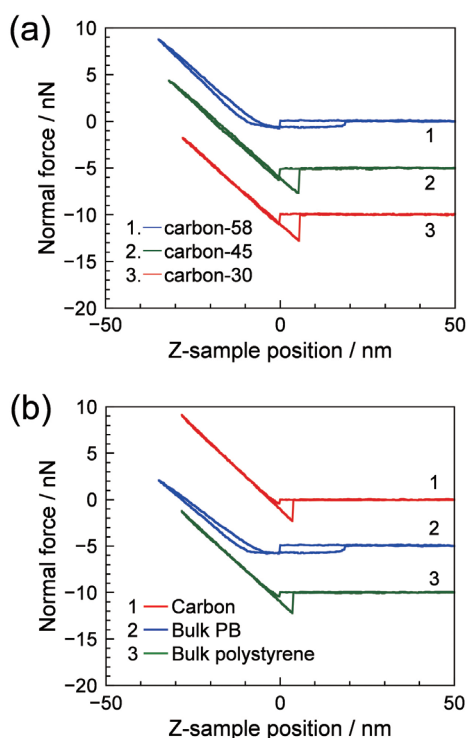


**Fig. 4:** Force-distance curve of BRL on carbon film, bulk PBD, bulk PS and carbon film.

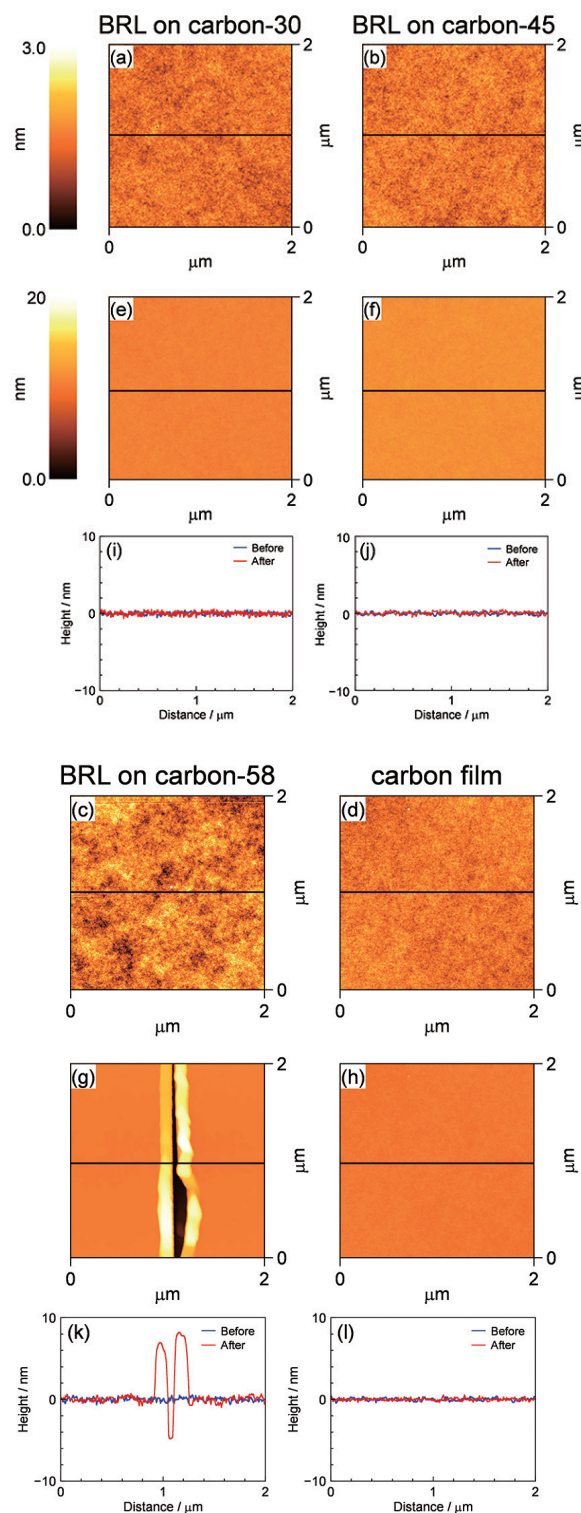


**Fig. 5:** Topographical AFM images of the RLs and carbon film (a–d) before and (e–h) after scratching. (i–l) Sectional view along the lines in the AFM images.

film. This indicates that the BRLs on hydrophobic carbons are not in a rubbery state, but are presumably in a glassy state, and their molecular motion is suppressed far above even the bulk glass transition temperature ( $T_g$ ).

Figure 5 summarizes the results of the wear test. As shown in Fig. 5(a–c), the BRL surfaces on carbon-30, carbon-45, and carbon-58 before scratching were flat with a root-mean-square roughness (RMS) of 0.3, 0.3, and 0.4 nm, respectively. These RMS values were almost identical to that obtained for the carbon film, 0.2 nm, shown in Fig. 5(d). After the wear test, a scratch track was observed at the surface of the BRL on carbon-58 (Fig. 5(g)), although the carbon film and the BRLs on carbon-30 and carbon-45 remained smooth (Fig. 5(e, f, and h)). The depth of the scratch was approximately 5 nm as shown in Fig. 5(k), which is comparable to the thickness of the BRL, 6.3 nm, as shown in Table 2. This indicates that almost all of the BRL was peeled off by scratching. Thus, we concluded that the BRLs on the hydrophobic carbons that have a high density and are not in a rubbery state showed good wear resistance, whereas the wear resistance of those on the hydrophilic carbons with a low density and in a rubbery state was poor.

#### Acknowledgements

The reported experiments were partially supported by the Photon and Quantum Basic Research Coordinated Development Program of MEXT.